

Ruthenium-Catalyzed Ring-Opening Polymerization Syntheses of Poly(organodecaboranes): New Single-Source Boron-Carbide Precursors

Xiaolan Wei, Patrick J. Carroll, and Larry G. Sneddon*

Department of Chemistry, University of Pennsylvania, Philadelphia, Pennsylvania 19104-6323

Received November 8, 2005. Revised Manuscript Received December 8, 2005

Ruthenium-catalyzed ring-opening metathesis polymerization (ROMP) of 6-R-B₁₀H₁₃ organodecaboranes containing strained-ring cyclic olefinic substituents has been found to be an important new method of generating poly(organodecaborane) polymers with higher molecular weights than previously attainable. The monomers, 6-(5-cyclooctenyl)-B₁₀H₁₃ (**1**), 6-(5-norbornenyl)-B₁₀H₁₃ (**2**), and 6-(4-cyclohexenyl)-B₁₀H₁₃ (**3**), were synthesized via the titanium-catalyzed decaborane hydroboration of 1 equiv of 1,5-cyclooctadiene, 2,5-norbornadiene, and 1,4-cyclohexadiene, respectively. The syntheses of the saturated, linked-cage compounds 6,6'-(1,5-cyclooctyl)-(B₁₀H₁₃)₂ (**4**) and 6,6'-(2,5-norbornyl)-(B₁₀H₁₃)₂ (**5**) were also achieved by either the titanium-catalyzed decaborane hydroboration of the remaining double bond of **1** or **2** or the titanium-catalyzed reactions of 1,5-cyclooctadiene and 2,5-norbornadiene with an excess amount of decaborane. ROMP of **1** and **2** using either of the Grubbs catalysts, Cl₂Ru(=CHPh)(PCy₃)L, L = PCy₃ (**I**) or H₂IMes (**II**), afforded the poly(6-cyclooctenyldecaborane) (PCD, **6**) and poly(6-norbornenyldecaborane) (PND, **7**) polymers. Molecular weights with *M_n* in excess of 30 kDa were readily obtained with polydispersities between 1.1 and 1.8. Both polymers are stable powders that are soluble in polar organic solvents. Studies of the ceramic conversion reactions of **6** and **7** using TGA, XRD, DRIFT, Raman, SEM, elemental analyses, and density measurements showed that they convert to boron-carbide/carbon ceramics upon pyrolysis. In accordance with their higher boron-to-carbon ratios, studies of the ceramic conversion reactions of compounds **4** and **5** showed them to be excellent single-source molecular precursors to boron-carbide ceramics with little or no excess carbon.

Introduction

Boron carbide is a highly refractory material of great interest for both its structural and its electronic properties.¹ Its chemical inertness, low density, high thermal stability, hardness, high cross-section for neutron capture, and excellent high-temperature thermoelectric properties give rise to numerous applications, including uses as an abrasive wear-resistant material, ceramic armor, and a neutron moderator in nuclear reactors and, potentially, for power generation in deep space flight applications.²

While boron-carbide powders are easily made by the direct reaction of the elements at high temperatures, new synthetic methods that allow the formation of pure boron carbide in processed forms still need to be developed. We have previously shown that both the poly(organodecaborane) polymers formed by the Cp₂Zr(CH₃)₂/B(C₆F₅)₃-catalyzed

polymerizations of alkenyldecaboranes and the bis-cage 6,6'-(CH₂)₆-(B₁₀H₁₃)₂ compound are excellent single-source precursors to boron-carbide ceramics.³ In this paper we report that the ruthenium-catalyzed ring-opening metathesis polymerization (ROMP) of alkenyldecaboranes containing strained cyclic olefinic substituents provides an important new route to poly(organodecaboranes) having higher molecular weights and narrower polydispersities than previously attainable.⁴ We also report our studies of the ceramic conversion reactions of these new polymers as well as two related hydrocarbon-bridged bis-decaborane compounds that show they are excellent single-source precursors to boron-carbide ceramic materials.

Experimental Section

All manipulations were carried out using standard high-vacuum or inert-atmosphere techniques as described by Shriver.⁵

- (1) For some recent reviews on the synthesis and properties of boron carbide, see: (a) Thevenot, F. *Key Eng. Mater.* **1991**, 56–57, 59–88. (b) *Boron Rich Solids*; Emin, D., Aselage, T., Beckel, C. L., Howard, I. A., Wood, C., Eds.; AIP Conf. Proc 140, Am. Inst. Phys.: New York, 1986. (c) *Boron Rich Solids*; Emin, D., Aselage, T., Switendick, A. C., Morosin, B., Beckel, C. L., Eds.; AIP Conf. Proc 231, Am. Inst. Phys.: New York, 1991.
- (2) (a) Wood, C. In *Boron Rich Solids*; Emin, D., Aselage, T., Beckel, C. L., Howard, I. A., Wood, C., Eds.; AIP Conf. Proc 140, Am. Inst. Phys.: New York, 1986; pp 362–372 and references therein. (b) Aselage, T. L.; Tallant, D. R.; Gieske, J. H.; Van Deusen, S. B.; Tissot, R. G. *Phys. Chem. Carbides, Nitrides Borides* **1990**, 97. (c) Aselage, T.; Emin, D. In *CRC Handbook of Thermoelectrics*; Rowe, D. M., Ed.; CRC Press: Boca Raton, 1995; pp 373–386.

- (3) (a) Pender, M. J.; Sneddon, L. G. *Polym. Prepr. (Am. Chem. Soc., Div. Polym. Chem.)* **2000**, 41, 551–552. (b) Pender, M. J.; Forsthoefel, K.; Sneddon, L. G. In *Group 13 Chemistry: Fundamental Research, Materials Science and Catalysis*; Shapiro, P., Atwood, D., Eds.; American Chemical Society Symposium Series; American Chemical Society: Washington, D.C., 2002; pp 168–180. (c) Sneddon, L. G.; Pender, M. J.; Forsthoefel, K.; Kusari, U.; Wei, X. *J. Eur. Ceram. Soc.* **2005**, 25, 91–97.
- (4) An initial communication has appeared: Wei, X.; Carroll, P. J.; Sneddon, L. G. *Organometallics* **2004**, 23, 163–165.
- (5) Shriver, D. F.; Drezdson, M. A. *The Manipulation of Air-Sensitive Compounds*, 2nd ed.; Wiley-Interscience: New York, 1996.

Materials. Decaborane was sublimed in vacuo prior to use. The 2,5-norbornadiene, 1,5-cyclooctadiene, ethylvinyl ether (Aldrich), and 1,4-cyclohexadiene (Acros) were dried over CaH_2 . CH_2Cl_2 (Fisher) was passed through an alumina drying column. The Grubbs catalysts $\text{Cl}_2\text{Ru}(\text{=CHPh})(\text{PCy}_3)_2$ (**1**) and $\text{Cl}_2\text{Ru}(\text{=CHPh})(\text{PCy}_3)(\text{H}_2\text{-Imes})$ (**II**) (H_2Imes = 1,3-dimesityl-4,5-dihydroimidazol-2-ylidene) from either Strem or Aldrich were used as received. ACS-grade hexanes, pentane, and silica gel with mesh sizes of 230–400 (Fisher) were used as received. C_6D_6 (D, 99.6%), CDCl_3 (D, 99.8%), and CD_2Cl_2 (D, 99.5%) (Cambridge Isotope Laboratories) were dried over 4 Å molecular sieves.

Physical Measurements. ^1H NMR spectra at 200.1 MHz and ^{11}B NMR spectra at 64.2 MHz were obtained on a Bruker AC 200 Fourier transform spectrometer. ^1H NMR spectra at 500.4 MHz and ^{11}B NMR spectra at 160.1 MHz were obtained on a Bruker AM 500 Fourier transform spectrometer. All ^{11}B NMR chemical shifts are referenced to external $\text{BF}_3\cdot\text{O}(\text{C}_2\text{H}_5)_2$ (0.00 ppm) with a negative sign indicating an upfield shift. All ^1H chemical shifts were measured relative to residual protons in the lock solvents and are referenced to Me_4Si (0.00 ppm). High-resolution mass spectra (HRMS) employing negative chemical ionization (NCI) were recorded on a Micromass Autospec spectrometer. Infrared spectra were recorded on a Perkin-Elmer 1430 Spectrometer using NaCl plates or a Perkin-Elmer 2000 FT-IR Spectrometer using KBr pellets. Diffuse reflectance infrared Fourier transform (DRIFT) spectra were obtained on a Mattson Galaxy FT-IR spectrometer at the University of New Mexico or on a Perkin-Elmer 2000 FT-IR Spectrometer with the DRIFT accessory at the University of Pennsylvania. The samples were prepared in a 6:1 KBr:ceramic ratio and recorded at a resolution of 4 cm^{-1} for 64 scans. FT-Raman spectra were obtained at Drexel University on a Renishaw RM1000 Raman Micro-Spectrometer with excitation using He–Ne 514 nm laser at a resolution of 1 cm^{-1} for 64 scans. Elemental analyses were performed at the analytical facility of the University of Pennsylvania or the Nesmeyanov Institute of Organoelement Compounds in Russia. In some of the ceramic analyses, the total analyses totaled less than 100%. This could indicate either incomplete combustion or oxygen contamination. Melting points were obtained on a standard melting point apparatus and uncorrected. Density measurements of the ceramics were carried out by flotation in halogenated solvents.

Molecular weights of the polymers were determined by gel permeation chromatography (GPC). The SEC-GPC instrument consisted of a Rainin HPLX solvent delivery system connected to Shodex GPC KF-801, KF-803, and KF-805 columns maintained at 40 °C. Two in-line detectors are connected in series, a Wyatt Technology mini-DAWN Tristar multi-angle laser light scattering detector with a 690-nm solid-state laser and a Wyatt Technology Optilab DSP interferometric refractometer operating at 690 nm. Tetrahydrofuran (THF) distilled over Na/benzophenone was used as the mobile phase and degassed in-line (Degasys DG-1210) prior to delivery to the GPC pump. The flow rate was 1 mL/min. Polymer solutions were prepared with ~5 mg/mL concentrations in THF. A loop size of 100 μL was employed, making each injection size 0.5 mg. The signals from the in-line detectors were analyzed using Astra 4.9.08 software from Wyatt Technology Corp. The dn/dc values (refractive index increment with concentration) of poly(6-cyclooctenyldecaborane) (**6**) (0.222 mL/g) and poly(6-norbornenyldecaborane) (**7**) (0.214 mL/g) at 690 nm were determined in THF using the Wyatt DNDC kit and analyzed with the DNDC software 5.90.03 from Wyatt Technology Corp.

Thermogravimetric analysis (TGA) was carried out on a Thermal Analysis SDT 2960 Simultaneous DTA-TGA. Glass-transition temperatures (T_g 's) of the polymers were measured on a Thermal

Analysis 2920 Differential Scanning Calorimeter with modulated DSC. Bulk pyrolyses of the ceramic precursors were carried out in a Lindberg model 54434 1700 °C tube furnace under a constant flow of Grade-5 argon that had been treated with an Oxyclear oxygen scavenger. A boron nitride boat containing the weighed sample was placed in the furnace in the center of a 1–1/8 in. alumina tube, heated at 10 °C/min, then held at temperature for the desired time before cooling back to room temperature at 10 °C/min.

Scanning electron microscopy (SEM) images were obtained with a JEOL 6300-FV high-resolution scanning electron microscope or a JEOL 6400 scanning electron microscope with a EDS (energy dispersive spectrometer). The samples were coated with gold and palladium. A working distance of 19 mm and an accelerating voltage of 10.0 kV were used. Powder X-ray diffraction (XRD) patterns were obtained with a Rigaku Geigerflex automated X-ray powder diffractometer using $\text{Cu K}\alpha$ ($\lambda = 1.5418\text{ Å}$) radiation and a graphite monochromator with a scan rate of 2°/min and a collection step of 0.1°.

6-(5-Cyclooctenyl)- $\text{B}_{10}\text{H}_{13}$ (1**).** In a procedure similar to that reported by Pender,⁶ in the glovebox, a 100 mL flask equipped with a stopcock and a magnetic stirring bar was charged with 64 mg (0.27 mmol) of $\text{Cp}_2\text{Ti}(\text{CO})_2$. The flask was then evacuated and back-filled with argon three times on a Schlenk line, and then, under an overpressure of argon, 0.60 g (4.9 mmol) of decaborane was added. The flask was sealed and subjected to three freeze–pump–thaw cycles on the high-vacuum line. Dry 1,5-cyclooctadiene (5.0 mL, 40 mmol) was condensed into the flask via static vacuum transfer. The flask was warmed to room temperature and then heated at 90 °C. A color change from brown to green was observed within 30 min. The reaction was complete in 21 h, at which time ^{11}B NMR analysis indicated the complete consumption of decaborane. The reaction mixture was then exposed to air and stirred for an additional 5 min. Column chromatography using hexanes eluent afforded 1.1 g (4.8 mmol, 96% yield) of **1** as a light-yellow oil, which gradually solidified into a waxy solid upon standing in vacuo. **1** was further purified via vacuum sublimation. $\text{Mp} = 41\text{--}42\text{ °C}$. NCI–HRMS (m/e): calcd for $^{12}\text{C}_8^{11}\text{B}_{10}\text{H}_{25}$ (M–H), 231.2887; found, 231.2885. Anal. Calcd for $\text{C}_8\text{B}_{10}\text{H}_{26}$: C, 41.71; H, 11.37. Found: C, 41.29; H, 11.67. ^{11}B NMR (160.1 MHz, CDCl_3 , ppm, $J = \text{Hz}$): 28.8 (s, 1, B6), 9.5 (d, 2, B1,3, J 154), 8.2 (d, 1, B9, J 163), 0.5 (d, 2, B5,7, J 153), –4.1 (d, 2, B8,10, J 152), –34.7 (d, 1, B2, J 151), –39.2 (d, 1, B4, J 158). ^1H NMR (500.4 MHz, CDCl_3 , ppm, $J = \text{Hz}$): 5.77 (d of t, 1H, J_1 18.2, J_2 7.7, =CH), 5.62 (d of t, 1H, J_1 16.7, J_2 9.8, =CH), 2.42 (m, 2H, =CHCH₂), 2.20 (m, 2H, =CHCH₂), 1.90 (m, 2H, CH₂), 1.78 (m, 2H, CH₂), 1.60 (m, 2H, CH₂), 1.44 (m, 1H, CH), –1.66 (s, br, 2H, BHB), –2.04 (s, br, 2H, BHB). IR (NaCl plate, cm^{-1}): 3000 (m), 2910 (vs), 2840 (s), 2550 (vs), 1900 (br, m), 1550 (m), 1490 (vs), 1460 (s), 1440 (m), 1355 (m), 1260 (w), 1180 (m), 1120 (w), 1100 (m), 1080 (w), 990 (vs), 950 (s), 925 (m), 895 (w), 870 (m), 850 (w), 820 (w), 800 (m), 780 (w), 750 (w), 715 (s), 675(s), 630 (m).

6-(5-Norbornenyl)- $\text{B}_{10}\text{H}_{13}$ (2**).** As described for **1**, 1.2 g (10 mmol) of decaborane, 6.0 mL (56 mmol) of 2,5-norbornadiene, and 70 mg (0.3 mmol) of $\text{Cp}_2\text{Ti}(\text{CO})_2$ were reacted at 90 °C for 96 h in vacuo. Column chromatography using hexanes eluent afforded 2.1 g (9.8 mmol, 98% yield) of **2** as a light-yellow oil, which crystallized in vacuo into colorless crystals. The *exo*-**2** was isolated by recrystallization from toluene at room temperature. $\text{Mp} = 41\text{--}42\text{ °C}$. NCI–HRMS (m/e): calcd for $^{12}\text{C}_7^{11}\text{B}_{10}\text{H}_{21}$ (M–H), 215.2574; found, 215.2577. Anal. Calcd for $\text{C}_7\text{B}_{10}\text{H}_{22}$: C, 39.22;

(6) (a) Pender, M. J.; Wideman, T.; Carroll, P. J.; Sneddon, L. G. *J. Am. Chem. Soc.* **1998**, *120*, 9108–9109. (b) Pender, M. J.; Carroll, P. J.; Sneddon, L. G. *J. Am. Chem. Soc.* **2001**, *123*, 12222–12231.

Table 1. ROMP Reactions of 6-(5-Cyclooctenyl)-B₁₀H₁₃ (**1**) Using **I** and **II**

	monomer, g/mmol	catalyst, mg/mmol	[M]/[Ru]	monomer recovered, g	monomer conver., %	polymer, g/yield, %	<i>M_n</i> /DP	<i>M_w</i>	PDI
I	0.112/0.48	4.2/5.1 × 10 ⁻³	95	0.041	63.4	0.057/809	12 500/54	16 400	1.31
I	0.102/0.44	8.7/1.1 × 10 ⁻²	42	0.045	56.0	0.046/810	6230/27	7820	1.26
II	0.143/0.62	4.5/5.1 × 10 ⁻³	117	0.029	80.0	0.110/961	32 580/141	57 730	1.77
II	0.126/0.55	8.0/9.4 × 10 ⁻³	58	0.034	73.4	0.084/908	21 150/91	29 350	1.40

Table 2. ROMP Reactions of 6-(5-norbornenyl)-B₁₀H₁₃ (**2**) Using **I** and **II**

	monomer, g/mmol	catalyst, mg/mmol	[M]/[Ru]	monomer recovered, g	monomer conver., %	polymer, g/yield, %	<i>M_n</i> /DP	<i>M_w</i>	PDI
I	0.111/0.52	4.2/5.1 × 10 ⁻³	101	0.006	94.7	0.094/89.4	31 200/145	34 970	1.12
I	0.115/0.53	8.3/9.8 × 10 ⁻³	53	0.014	88.2	0.087/85.9	19 200/89	21 080	1.10
II	0.126/0.59	4.5/5.1 × 10 ⁻³	111	0.008	94.0	0.103/86.8	31 950/148	52 050	1.63
II	0.119/0.55	8.1/9.5 × 10 ⁻³	58	0.013	89.2	0.095/89.7	23 660/110	33 150	1.40

H, 10.34. Found: C, 38.55; H, 10.10. ¹B NMR (160.1 MHz, CDCl₃, ppm, *J* = Hz): 25.9 (s, 1, B6), 8.2 (d, 2, B1,3, *J* 146), 6.6 (d, 1, B9, *J* 161), -0.8 (d, 2, B5,7, *J* 149), -5.3 (d, 2, B8,10, *J* 150), -35.7 (d, 1, B2, *J* 152), -40.6 (d, 1, B4, *J* 157). ¹H NMR (500.4 MHz, CDCl₃, ppm, *J* = Hz): 6.20 (d of t, 1H, *J*₁ 5.6, *J*₂ 2.6, =CH), 6.06 (d of t, 1H, *J*₁ 5.6, *J*₂ 3.0, =CH), 2.97 (d, 2H, *J* 11.8, =CHCH), 1.75 (m, 2H, CH₂), 1.49 (m, 1H, CH), 1.37 (m, 1H, CH), 1.30 (m, 1H, CH), -1.50 (s, br, 2H, BHB), -2.00 (s, br, 2H, BHB). IR (NaCl plate, cm⁻¹): 3045 (s), 2950 (vs), 2860 (s), 2550 (vs), 1900 (br, m), 1540 (m), 1500 (s), 1440 (s), 1330 (s), 1280 (m), 1220 (m), 1180 (w), 1130 (m), 1090 (s), 1000 (s), 970 (m), 930 (m), 915 (m), 860 (m), 820 (w), 780 (w), 770 (w), 710 (s), 685(m), 660 (m).

6-(4-Cyclohexenyl)-B₁₀H₁₃ (3**).** As described for **1**, 2.0 g (16.4 mmol) of decaborane, 4.0 mL (41.9 mmol) of 1,4-cyclohexadiene, and 96 mg (0.5 mmol) of Cp₂Ti(CO)₂ were heated at 90 °C for 36 h in vacuo. Column chromatography with hexanes eluent afforded 3.1 g (15.3 mmol, 94% yield) of **3** as white needles. Mp = 53–55 °C. NCI–HRMS (*m/e*): calcd for ¹²C₆¹¹B₁₀¹H₂₁ (M–H), 203.2574; found, 203.2571. Anal. Calcd for C₆B₈H₂₂: C, 35.62; H, 10.96. Found: C, 35.25; H, 11.44. ¹B NMR (160.1 MHz, CDCl₃, ppm, *J* = Hz): 23.9 (s, 1, B6), 8.4 (d, 2, B1,3, *J* 147), 6.7 (d, 1, B9, *J* 158), -0.9 (d, 2, B5,7, *J* 148), -4.7 (d, 2, B8,10, *J* 151), -35.9 (d, 1, B2, *J* 153), -40.6 (d, 1, B4, *J* 148). ¹H NMR (500.4 MHz, CDCl₃, ppm): 5.74 (m, 2H, =CH), 2.27 (m, 2H, CH₂), 2.12 (m, 2H, CH₂), 2.07 (m, 2H, CH₂), 1.63 (m, 1H, CH), -1.67 (s, br, 2H, BHB), -2.02 (s, br, 2H, BHB). IR (NaCl plate, cm⁻¹): 3005 (m), 2900 (s), 2815 (s), 2560 (vs), 1895 (w), 1640 (w), 1545 (m), 1530 (w), 1490 (s), 1425 (s), 1385 (w), 1345 (w), 1280 (w), 1255 (w), 1190 (m), 1180 (w), 1135 (m), 1095 (s), 950 (m), 915 (m), 895 (m), 855 (w), 835 (w), 805 (m), 745 (w), 715 (w), 675 (m), 645 (s), 635 (m).

6,6'-(1,5-Cyclooctyl)-(B₁₀H₁₃)₂ (4**).** As described for **1**, 1.6 g (13 mmol) of decaborane, 2.5 g (11 mmol) of **1**, and 114 mg (0.5 mmol) of Cp₂Ti(CO)₂ in 5 mL of dry benzene were reacted at 90 °C until the ¹H NMR analysis showed the complete consumption of the olefin (120 h). The reaction mixture was then exposed to air. Column chromatography with stepwise hexanes and benzene elutions afforded 3.5 g (10 mmol, 91% yield) of **4** as a white powder. Mp = 102–105 °C. NCI–HRMS (*m/e*): calcd for ¹²C₈¹¹B₂₀¹H₃₉ (M–H), 355.4913; found, 355.4905. Anal. Calcd for C₈B₂₀H₄₀: C, 27.25; H, 11.43. Found: C, 27.34; H, 12.06. ¹B NMR (160.1 MHz, CDCl₃/CD₂Cl₂, ppm, *J* = Hz): 27.8 (s, 1, B6), 9.8 (d, 2, B1,3, *J* 147), 8.2 (d, 1, B9, *J* 157), 0.6 (d, 2, B5,7, *J* 150), -3.8 (d, 2, B8,10, *J* 151), -34.7 (d, 1, B2, *J* 153), -39.0 (d, 1, B4, *J* 154). ¹H NMR (500.4 MHz, CDCl₃/CD₂Cl₂, ppm): 2.03 (m, 2H), 1.89 (m, 8H), 1.64 (m, 4H), -1.69 (s, br, 4H, BHB), -2.02 (s, br, 4H, BHB). FT-IR (KBr pellet, cm⁻¹): 2925 (s), 2850 (m), 2577 (vs), 1901 (w), 1500 (s), 1424 (s), 1103 (w), 1003 (m), 959 (w), 933 (w), 884 (w), 861 (w), 840 (w), 814 (w), 721 (m), 685 (m), 524 (w).

6,6'-(2,5-Norbornyl)-(B₁₀H₁₃)₂ (5**).** As described for **4**, 1.5 g (12 mmol) of decaborane, 2.0 g (9.3 mmol) of **2**, and 175 mg (0.75 mmol) of Cp₂Ti(CO)₂ were reacted in 5 mL of benzene at 90 °C for 72 h in vacuo. Column chromatography using stepwise hexanes and benzene elutions followed by recrystallization from cold hexanes afforded 2.1 g (6.2 mmol, 67% yield) of **5** as a white solid. Mp = 170–171 °C. NCI–HRMS (*m/e*): calcd for ¹²C₇¹¹B₂₀¹H₃₅ (M–H), 339.4600; found, 339.4589. Anal. Calcd for C₇B₂₀H₃₆: C, 24.98; H, 10.78. Found: C, 25.53; H, 10.80. ¹B NMR (160.1 MHz, CDCl₃, ppm, *J* = Hz): 25.3 (s, 1, B6), 8.3 (d, 2, B1,3, *J* 148), 6.9 (d, 1, B9, *J* 146), -0.7 (d, 2, B5,7, *J* 150), -5.2 (d, 2, B8,10, *J* 151), -35.9 (d, 1, B2, *J* 154), -40.3 (d, 1, B4, *J* 155). ¹H NMR (500.4 MHz, CDCl₃, ppm): 2.51 (m, 2H), 1.74 (m, 4H), 1.61 (m, 2H), 1.51 (m, 2H), -1.60 (s, br, 4H, BHB), -2.00 (s, br, 4H, BHB). FT-IR (KBr pellet, cm⁻¹): 2954 (s), 2869 (m), 2580 (vs), 2525 (m), 1902 (w), 1504 (m), 1419 (w), 1322 (w), 1275 (w), 1144 (w), 1102 (w), 1007 (m), 995 (w), 962 (w), 928 (m), 860 (w), 812 (w), 770 (w), 730 (w), 719 (w), 685 (m), 501 (w).

Poly(6-cyclooctenyldecaborane) (PCD, **6).** In the glovebox, the desired amount of catalyst **I** or **II** was added to a two-neck round-bottom flask equipped with a vacuum adapter, a magnetic stir bar, and a septum. The flask was evacuated on a Schlenk line and then back filled with argon for three pump–fill cycles. Dry CH₂Cl₂ (3 mL) was added to dissolve the catalyst. A weighed sample of 6-(5-cyclooctenyl)-B₁₀H₁₃ (**1**) was degassed, dissolved in 7 mL of CH₂-Cl₂, and then added to the stirring catalyst solution through the septum. The reaction mixture was either stirred for 1 h at room temperature (for **I**) or heated at gentle reflux (for **II**). The reaction mixture was exposed to air and quenched with 1 mL of ethylvinyl ether and then stirred for an additional 5 min. Column chromatography with pentane eluted unreacted monomer. Elution with CH₂-Cl₂ afforded the polymer. The waxy off-white polymer PCD (**6**) was then precipitated by adding the concentrated CH₂Cl₂ solution to vigorously stirred pentane. The details for each reaction are summarized in Table 1. Anal. Calcd for C₈B₁₀H₂₆: C, 41.71; H, 11.37. Found: C, 42.25; H, 11.34. ¹B{¹H} NMR (64.2 MHz, CD₂-Cl₂, ppm): 28.1 (s, br, 1, B6), 11.6 (s, 3, B1,3 and B9), 2.5 (s, 2, B5,7), -1.7 (s, 2, B8,10), -32.2 (s, 1, B2), -36.8 (s, 1, B4). ¹H NMR (200.1 MHz, CD₂Cl₂, ppm): 5.44–5.25 (m, 2H), 2.03 (m, 4H), 1.54 (m, 6H), 1.42 (s, 1H), -1.7 (br, 2BHB), -2.0 (br, 2BHB). IR (NaCl plate, cm⁻¹): 3620 (s), 2900 (vs), 2830 (vs), 2550 (vs), 1900 (br, m), 1550 (m), 1490 (s), 1425 (s), 1355 (m), 1305 (m), 1250 (s), 1220 (m), 1205 (w), 1150 (m), 990 (s), 955 (m), 925 (w), 910 (w), 895 (w), 885 (w), 860 (w), 850 (w), 800 (m), 730 (s), 700 (m), 675 (m).

Poly(6-norbornenyldecaborane) (7**).** PND (**7**) was synthesized in a similar manner as described for PCD (**6**). The workup included the elimination of the residue catalyst by filtering through a short silica gel plug and precipitation from a stirred pentane solution to afford PND (**7**) as an off-white powder. The details for each reaction are summarized in Table 2. ¹B{¹H} NMR (64.2 MHz, CD₂Cl₂,

Table 3. Crystallographic Data Collection and Structural Refinement Information

	2	3	5
empirical formula	C ₇ B ₁₀ H ₂₂	C ₆ B ₁₀ H ₂₂	C ₇ B ₂₀ H ₃₆
fw	214.35	202.34	336.56
cryst class	monoclinic	orthorhombic	monoclinic
space group	<i>P</i> 2 ₁ / <i>c</i> (#14)	<i>Pca</i> 2 ₁ (#29)	<i>P</i> 2 ₁ / <i>c</i> (#14)
<i>Z</i>	4	8	4
<i>a</i> , Å	10.906(2)	10.969(4)	12.1819(2)
<i>b</i> , Å	13.048(2)	21.912(8)	15.9470(3)
<i>c</i> , Å	10.811(2)	10.902(4)	11.0751(2)
α , deg			
β , deg	117.287(3)		90.056(1)
γ , deg			
<i>V</i> , Å ³	1367.3(5)	2620(2)	2151.50(7)
μ , cm ⁻¹	0.47	0.45	0.44
crys size, mm	0.38 × 0.15 × 0.12	0.48 × 0.08 × 0.02	0.36 × 0.20 × 0.08
<i>D</i> _{calcd} , g/cm ³	1.041	1.026	1.039
<i>F</i> (000)	456	864	712
radiation	Mo K α	Mo K α	Mo K α
2 θ angle, deg	5.24–50.7	5.26–50.7	5.1–50.7
temp, K	143	143	180
<i>hkl</i> collected	–11 ≤ <i>h</i> ≤ 12 –15 ≤ <i>k</i> ≤ 12 –10 ≤ <i>l</i> ≤ 12	–13 ≤ <i>h</i> ≤ 11 –26 ≤ <i>k</i> ≤ 23 –10 ≤ <i>l</i> ≤ 13	–14 ≤ <i>h</i> ≤ 14 –19 ≤ <i>k</i> ≤ 18 –13 ≤ <i>l</i> ≤ 13
no. reflns measd	7237	8440	16 287
no. unique reflns	2430 (<i>R</i> _{int} = 0.0224)	3830 (<i>R</i> _{int} = 0.1102)	3866 (<i>R</i> _{int} = 0.0523)
no. obsd reflns (<i>F</i> > 4 σ)	2019	2439	3517
no. reflns used in refinement	2430	3830	3866
no. params	230	290	395
<i>R</i> ^a indices (<i>F</i> > 4 σ)	<i>R</i> ₁ = 0.0763 <i>wR</i> ₁ = 0.2025	<i>R</i> ₁ = 0.1290 <i>wR</i> ₁ = 0.2905	<i>R</i> ₁ = 0.0707 <i>wR</i> ₁ = 0.1393
<i>R</i> ^a indices (all data)	<i>R</i> ₁ = 0.0892 <i>wR</i> ₂ = 0.2171	<i>R</i> ₁ = 0.1600 <i>wR</i> ₂ = 0.3198	<i>R</i> ₁ = 0.0798 <i>wR</i> ₂ = 0.1464
GOF ^b	1.066	1.044	1.131
final difference peaks, e/Å ³	+0.489, –0.257	+0.464, –0.395	+1.148, –0.177

^a *R*₁ = $|F_o| - |F_c|/|F_o|$; *wR*₂ = $\{w(F_o^2 - F_c^2)^2/w(F_o^2)^2\}^{1/2}$. ^b GOF = $\{w(F_o^2 - F_c^2)^2/(n - p)\}^{1/2}$, where *n* = number of reflections and *p* = number of parameters refined.

ppm): 30.1 (s, br, 1, B6), 12.4 (s, 3, B1,3,9), 3.3 (s, 2, B5,7), –0.8 (s, 2, B8,10), –31.5 (d, 1, B2), –36.3 (d, 1, B4). ¹H NMR (200.1 MHz, CD₂Cl₂, ppm): 5.30 (m, 2H), 2.64 (m, 1H), 1.99 (m, 1H), 1.81 (m, 1H), 1.55 (m, 2H), 1.26 (m, 2H), –1.60 (br, 2BHB), –1.98 (br, 2BHB). Anal. Calcd for C₇B₁₀H₂₂: C, 39.22; H, 10.34. Found: C, 40.28; H, 10.79. IR (NaCl plate, cm⁻¹): 3350 (m), 2950 (vs), 2870 (vs), 2580 (vs), 2320 (s), 2210 (s), 1900 (br, s), 1750 (w), 1560 (s), 1500 (vs), 1430 (s), 1310 (m), 1100 (m), 1010 (s), 960 (s), 940 (m), 860 (m), 810 (s), 720 (s), 710 (s), 690 (s).

Crystallographic Data for 2, 3, and 5. Single crystals of **exo-2** (Upenn #3212) and **5** (Upenn #3193) were grown from toluene solutions at room temperature. Single crystals of **3** (Upenn #3250) were obtained via sublimation in vacuo onto a –45 °C coldfinger.

Collection and Reduction of the Data. X-ray intensity data were collected on a Rigaku Mercury CCD area detector employing graphite-monochromated Mo K α (λ = 0.71069 Å) radiation at a temperature of 143 K for **2** and **3** and on a Rigaku R-Axis IIC area detector employing graphite-monochromated Mo K α at a temperature of 180 K for **5**. Intensity data for **2** and **3** were measured using 0.5° rotations with exposures of 90 and 120 s, respectively. Intensity data for **5** were measured using 0.5° oscillations and exposures of 1200 s. Rotation images for **2** and **3** were processed using CrystalClear,⁷ producing a listing of unaveraged *F*² and $\sigma(F^2)$ values which were then passed to the CrystalStructure program package⁸ for further processing and structure solution on a Dell Pentium III computer. Oscillation images for **5** were processed using BioteX,⁹ producing a listing of unaveraged *F*² and $\sigma(F^2)$ values

which were then passed to the teXsan program package¹⁰ for further processing and structure solution on a Silicon Graphic Indigo R4000 computer. The intensity data were corrected for Lorentz and polarization effects. Absorption corrections were made for **2** and **3** using REQAB.¹¹

Solution and Refinement of the Structures. The crystallographic data collection parameters and refinement data for **2**, **3**, and **5** are summarized in Table 3. The structures were solved by direct methods (SIR97).¹² Refinements were by full-matrix least squares based on *F*² using SHELXL-97¹³ (**2** and **3**) or SHELXL-93 (**5**).¹⁴ All reflections were used during refinement (*F*²'s that were experimentally negative were replaced by *F*² = 0). In all structures, non-hydrogen atoms were refined anisotropically. In **2** and **5**, the cage hydrogen atoms were refined isotropically and the norbornene and norbornane hydrogens refined using a riding model. In **3**, the cage hydrogens were not refined and the cyclohexene hydrogens were refined using a riding model. In **2**, the norbornenyl disorder involves the superposition of both enantiomers of norbornene in a

(7) CrystalClear; Rigaku Corp.: 1999.

(8) CrystalStructure: Crystal Structure Analysis Package; Rigaku Corp.: 2002.

(9) BioteX: A suite of Programs for the Collection, Reduction and Interpretation of Imaging Plate Data; Molecular Structure Corp.: 1995.

(10) teXsan: Crystal Structure Analysis Package; Molecular Structure Corp.: 1985 and 1992.

(11) REQAB; Jacobsen, R. A. Private Communication, 1994.

(12) SIR97: Altomare, A.; Burla, M. C.; Camalli, M.; Cascarano, G.; Giacovazzo, C.; Moliterni, A.; Polidori, G.; Spagna, R. *J. Appl. Crystallogr.* **1999**, 32, 115–119.

(13) SHELXL-97: Sheldrick, G. M. *SHELXL-97, Program for the Refinement of Crystal Structures*; University of Göttingen: Göttingen, Germany, 1997.

(14) SHELXL-93: Sheldrick, G. M. *SHELXL-93, Program for the Refinement of Crystal Structures*; University of Göttingen: Göttingen, Germany, 1993.

ratio of 0.70/0.30; in **5**, the norbornyl disorder involves both enantiomers of norbornane in a 0.535/0.465 ratio.

Results and Discussion

Metal-catalyzed ring-opening metathesis polymerization reactions of strained olefins using either "Schrock-type"¹⁵ $M(\text{NAr})(=\text{CHR})(\text{OR}')_2$, $M = \text{Mo}, \text{W}$, or "Grubbs-type" $\text{Cl}_2\text{-Ru}(=\text{CHPh})(\text{PCy}_3)_2\text{L}$, $\text{L} = \text{PCy}_3$ (**I**) or H_2IMes (**II**), catalysts¹⁶ have been applied to the ROMP of a variety of ring systems including norbornenes, norbornadienes, 7-oxanorbornenes, cyclooctatetraenes, and cyclooctadienes and can generate organic polymers with highly monodispersed and controllable molecular weights.¹⁷ There have also been examples of the use of ROMP methods to produce inorganic polymers. For example, Chung showed that $\text{WCl}_6/\text{Me}_4\text{Sn}$ catalyzed ROMP of 9-BBN-norbornene to poly(9-BBN-norbornene) and that $\text{W}(=\text{CH}^t\text{Bu})(\text{NAr})[\text{OCMe}(\text{CF}_3)_2]_2$ catalyzed the formation of poly(5-cyclooctenyldiethylborane) by ROMP of (5-cyclooctenyl)diethylborane.¹⁸ Allcock also utilized the $\text{Cl}_2\text{Ru}(=\text{CHPh})(\text{PCy}_3)_2$ catalyst for the ROMP of phosphazene-functionalized norbornenes.¹⁹ These prior results suggested to us that metal-catalyzed ROMP reactions of decaborane-functionalized cyclic olefins could be employed as a route to new classes of poly(organodecaborane) polymers.

Monomer Syntheses via Titanium-Catalyzed Hydroboration of Cyclic Dienes. Following on an earlier report by Hartwig on the titanium-catalyzed hydroboration of olefins by catecholborane,²⁰ Pender showed⁶ that $\text{Cp}_2\text{Ti}(\text{CO})_2$ catalyzes the hydroboration of terminal olefins by decaborane to produce 6-R- $\text{B}_{10}\text{H}_{13}$ organodecaborane derivatives in high yields. As shown in eqs 1–3, using a similar procedure, the $\text{Cp}_2\text{Ti}(\text{CO})_2$ -catalyzed hydroboration reactions of decaborane with the cyclic-dienes 1,5-cyclooctadiene, 2,5-norbornadiene, and 1,4-cyclohexadiene were found to afford the corresponding 6-substituted derivatives 6-(5-cyclooctenyl)- $\text{B}_{10}\text{H}_{13}$ (**1**),

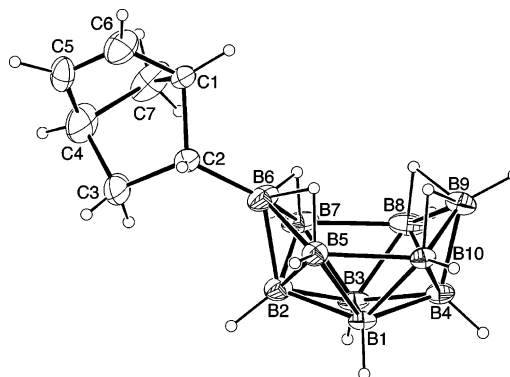
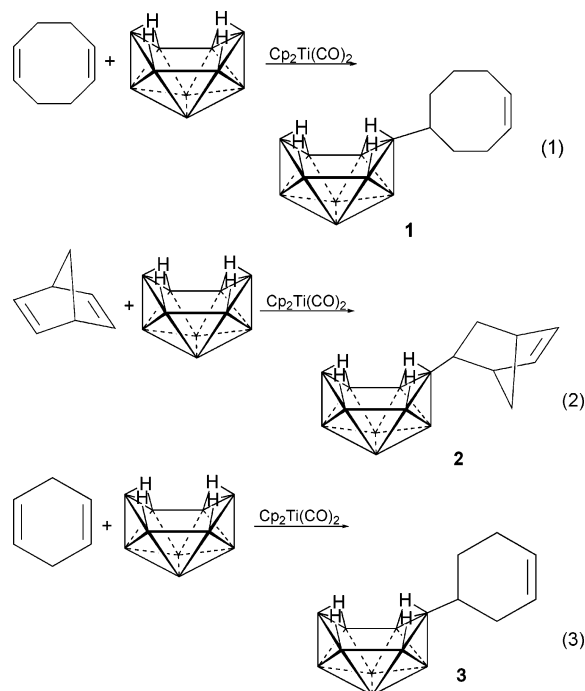


Figure 1. ORTEP representation of the structure of *exo*-6-(5-norbornenyl)- $\text{B}_{10}\text{H}_{13}$ (**2**). Selected bond lengths (Å) and angles (deg): C1–C2, 1.568(4); C2–C3, 1.539(8); C3–C4, 1.494(8); C4–C5, 1.460(4); C5–C6, 1.259(5); C1–C7, 1.610(8); C4–C7, 1.571(7); C2–B6, 1.613(5); B5–B6, 1.792(4); B6–B7, 1.819(4); C1–C2–C3, 102.3(3); C2–C3–C4, 103.9(4); C3–C4–C5, 109.9(4); C3–C4–C7, 101.6(4); C4–C5–C6, 112.6(3); C1–C6–C5, 106.6(4); C7–C1–C2, 99.6(3); C1–C7–C4, 89.2(3); C6–C1–C2, 108.5(3); C6–C1–C7, 99.5(3); C1–C2–B6, 113.6(3); C3–C2–B6, 116.0(4); C2–B6–B2, 128.6(3); C2–B6–B5, 121.8(3); C2–C6–B7, 132.6(2).

6-(5-norbornenyl)- $\text{B}_{10}\text{H}_{13}$ (**2**), and 6-(4-cyclohexenyl)- $\text{B}_{10}\text{H}_{13}$ (**3**) in nearly quantitative yields (96% for **1**, 98% for **2**, and 94% for **3**).



In a typical reaction, a mixture of decaborane, excess diene, and the $\text{Cp}_2\text{Ti}(\text{CO})_2$ catalyst was heated at 90 °C in vacuo. A characteristic color change from brown to green was observed within 30 min. The reactions were monitored by $^{11}\text{B}\{^1\text{H}\}$ NMR and stopped when the starting decaborane was completely consumed. Vacuum evaporation of the excess diene followed by separation of the metal residue using column chromatography with hexanes eluent yielded **1**, **2**, and **3** as white solids. The compounds were soluble in a range of nonpolar and polar organic solvents including hexanes, benzene, toluene, methylene chloride, and chloroform. They were stable under inert atmosphere but slowly hydrolyzed in air.

- (15) (a) Schrock, R. R. *Acc. Chem. Res.* **1990**, *23*, 158–165. (b) Schrock, R. R.; Murdzek, J. S.; Bazan, G. C.; Robbins, J.; Dimare, M.; O'Regan, M. J. *Am. Chem. Soc.* **1990**, *112*, 3875–3886. (c) Bazan, G. C.; Khosravi, E.; Schrock, R. R.; Feast, W. J.; Gibson, V. C.; O'Regan, M. B.; Thomas, J. K.; Davis, W. M. *J. Am. Chem. Soc.* **1990**, *112*, 8378–8387. (d) Bazan, G. C.; Oskam, J. H.; Cho, H. N.; Park, L. Y.; Schrock, R. R. *J. Am. Chem. Soc.* **1991**, *113*, 6899–6907.
- (16) (a) Schwab, P.; Grubbs, R. H.; Ziller, J. W. *J. Am. Chem. Soc.* **1996**, *118*, 100–110. (b) Scholl, S.; Ding, S.; Lee, C. W.; Grubbs, R. H. *Org. Lett.* **1999**, *1*, 953–956. (c) Sanford, M. S.; Love, J. A.; Grubbs, R. H. *J. Am. Chem. Soc.* **2001**, *123*, 6543–6554. (d) Trnka, T. M.; Grubbs, R. H. *Acc. Chem. Res.* **2001**, *34*, 18–29.
- (17) For general reviews of ROMP, see: (a) *Olefin Metathesis and Ring-Opening Polymerization of Cycloolefins*; Dragutan, V., Balaban, A. T., Dimonie, M., Eds.; Wiley: Chichester, U.K., 1985. (b) *Olefin Metathesis and Metathesis Polymerization*, 2nd ed.; Ivin, K. J., Mol, I. C., Eds.; Academic: New York, 1986. (c) *Catalytic Polymerization of Cycloolefins: Ionic, Ziegler–Natta and Ring-Opening Metathesis Polymerization*; Dragutan, V., Streck, R., Eds.; Elsevier: New York, 2000. (d) Grubbs, R. H. *Handbook of Metathesis*; Wiley-VCH: Weinheim, 2003. (e) Grubbs, R. H.; Tumas, W. *Science* **1989**, *243*, 907–915. (f) Buchmeiser, M. R. *Chem. Rev.* **2000**, *100*, 1565–1604. (g) Ivin, K. J. *J. Mol. Catal. A: Chem.* **2004**, *213*, 39–45.
- (18) (a) Ramakrishna, S.; Chung, T. C. *Macromolecules* **1989**, *22*, 3181–3183. (b) Ramakrishna, S.; Chung, T. C. *Macromolecules* **1990**, *23*, 4519–4527. (c) Chung, T. C.; Ramakrishna, S.; Kim, M. W. *Macromolecules* **1991**, *24*, 2675–2681. (d) Chung, T. C. *J. Mol. Catal.* **1992**, *76*, 15–31.
- (19) Allcock, H. R.; Laredo, W. R.; deDenus, C. R.; Taylor, J. P. *Macromolecules* **1999**, *32*, 7719–7725.
- (20) He, X.; Hartwig, J. F. *J. Am. Chem. Soc.* **1996**, *118*, 1696–1702.

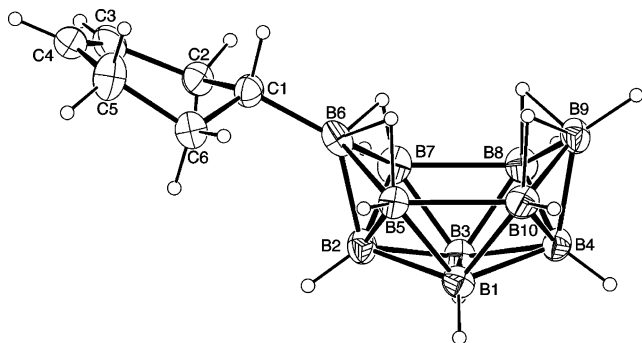
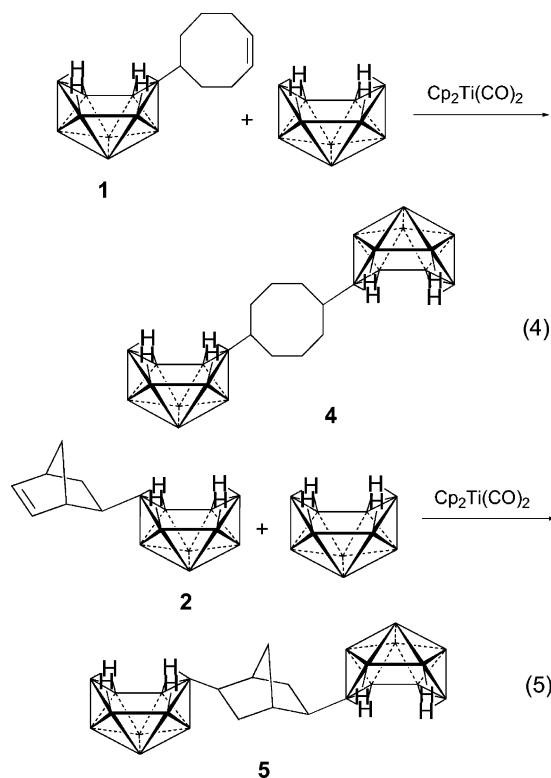


Figure 2. ORTEP representation of the structure of 6-(4-cyclohexenyl)- $B_{10}H_{13}$ (**3**). Selected bond lengths (Å) and bond angles (deg): C1–C2, 1.545(8); C2–C3, 1.475(9); C3–C4, 1.344(10); C4–C5, 1.456(10); C5–C6, 1.524(9); C1–C6, 1.495(9); B2–B6, 1.745(11); B5–B6, 1.790(10); B6–B7, 1.827(9); C1–C2–C3, 113.1(5); C2–C3–C4, 122.5(6); C3–C4–C5, 124.2(6); C4–C5–C6, 112.8(6); C5–C6–C1, 112.9(6); C2–C1–C6, 113.7(5); C1–B6–B2, 131.5(5); C1–B6–B5, 127.2(5); C1–B6–B7, 128.5(5).

The ^{11}B NMR spectra of all three compounds showed similar 1:2:1:2:2:1:1 patterns, consisting of a broad low-field singlet at ~ 27 ppm, assigned to the B6 atom attached to the organo substituent, and six doublet resonances that are typical of 6-R- $B_{10}H_{13}$ derivatives.²¹ Their 1H NMR spectra showed the resonances characteristic of their organic fragments, the broad overlapping peaks of the terminal B–H's, and two sets of intensity-two decaborane bridging-hydrogen resonances. Although Brown reported that the hydroboration of norbornadiene by 9-BBN afforded only the *exo*-9-BBN-norbornene isomer,²² both the *exo* and *endo* isomers of **2** were formed in a 4:1 ratio, as determined by the integration of their vinyl resonances. Resonances observed in the 120–130 ppm region of the ^{13}C NMR spectra of **1**, **2**, and **3** confirm the presence of carbon–carbon double bonds. Their FT-IR spectra showed the broad B–H stretching bands at $\sim 2600\text{ cm}^{-1}$ in addition to the absorptions characteristic of their olefinic substituents.

The structures of *exo*-6-(5-norbornenyl)- $B_{10}H_{13}$ (**2**) and 6-(4-cyclohexenyl)- $B_{10}H_{13}$ (**3**) were confirmed by single-crystal X-ray crystallography. The norbornenyl unit of **2** was disordered with two orientations in a 0.7/0.3 ratio; therefore, the bond lengths and angles must be viewed with caution. The ORTEP representation of the major (70%) orientation displayed in Figure 1 confirms a 6-substituted norbornenyl–decaborane structure resulting from the titanium-catalyzed hydroboration of the norbornadiene C2–C3 double bond. The observed C2–C3 (1.539(8) Å) and C5–C6 (1.259(5) Å) bond lengths are consistent with carbon–carbon single and double bonds, respectively. As shown in Figure 2, the six-membered cyclohexenyl ring in **3** adopts a puckered structure with the C1 and C6 methylene carbons lying above and below the C5–C4–C3–C2 plane. The C1–C2 bond length (1.545(8) Å) is consistent with a single bond resulting from hydroboration of the original C1–C2 double bond of 1,4-hexadiene. The C3–C4 bond length (1.344(10) Å) and C2–C3–C4 (122.5(6)°) and C3–C4–C5 (124.2(6)°) bond angles confirm a double bond between C3 and C4. The remaining bond lengths and angles in **2** and **3** fall in the normal ranges.

The $Cp_2Ti(CO)_2$ -catalyzed reactions (eqs 4 and 5) of **1** and **2** with 1 equiv of decaborane afforded the saturated, hydrocarbon-bridged compounds 6,6'-(1,5-cyclooctyl)-($B_{10}H_{13}$)₂ (**4**) and 6,6'-(2,5-norbornyl)-($B_{10}H_{13}$)₂ (**5**) in 91% and 67% yields, respectively. Alternatively, the $Cp_2Ti(CO)_2$ -catalyzed reaction of 2 equiv of decaborane with 1,5-cyclooctadiene and 2,5-norbornadiene can also be used to produce **4** and **5**. The products were isolated from excess decaborane and any metal residue via column chromatography using hexanes and benzene eluents. Further purification by recrystallization from CH_2Cl_2 /hexanes solution yielded **4** and **5** as white powders that were soluble in benzene, toluene, and methylene chloride but only sparingly soluble in hexanes. They were stable under inert atmosphere but slowly hydrolyzed in air.



The ^{11}B NMR spectra of **4** and **5** were nearly identical to those of **1**–**3**, again showing a 1:2:1:2:2:1:1 pattern composed of a downfield singlet for B6 and six sets of doublets.²¹ Their 1H NMR spectra showed, in addition to the two sets of broad intensity-four resonances for the decaborane bridging hydrogens, that the downfield olefinic resonances of **1** and **2** had been replaced by upfield alkyl resonances. Likewise, the $C=C$ bond stretch observed near 1550 cm^{-1} in the FT-IR spectra of **1** and **2** was absent in the spectra of **4** and **5**.

A single-crystal X-ray diffraction study (Figure 3) confirmed a linked-cage structure for **5** in which the two decaborane cages are bonded to the C2 and C5 norbornyl carbons as a result of decaborane hydroboration of the C2–C3 and C5–C6 double bonds of norbornadiene. The molecule processes C_{2v} symmetry having a 2-fold rotation axis through C7, with the two mirror planes containing C1–

(21) Todd, L. J.; Siedle, A. R. *Prog. NMR Spectrosc.* **1993**, *13*, 87–176.

(22) Brown, H. C.; Liotta, R.; Kramer, G. W. *J. Org. Chem.* **1978**, *43*, 1058–1063.

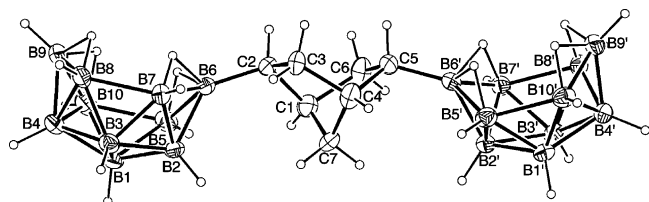
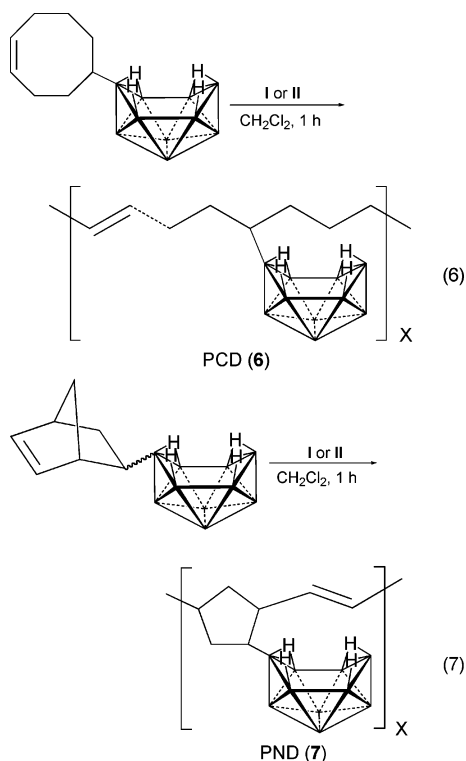


Figure 3. ORTEP representation of the structure of 6,6'-(2,5-norbornyl)-(B₁₀H₁₃)₂ (**5**). Selected bond lengths (Å) and bond angles (deg): C1–C2, 1.564(9); C2–C3, 1.551(9); C3–C4, 1.524(9); C4–C5, 1.608(6); C5–C6, 1.402(7); C1–C6, 1.563(10); C1–C7, 1.459(11); C4–C7, 1.552(11); C2–B6, 1.574(4); C5–B6', 1.570(4); C1–C2–C3, 101.5(4); C2–C3–C4, 106.3(6); C3–C4–C5, 107.5(5); C4–C5–C6, 105.2(4); C5–C6–C1, 107.5(5); C2–C6–C1, 105.5(6); C1–C7–C4, 99.2(6); C2–C1–C7, 102.7(6); C6–C1–C7, 98.0(7); C3–C4–C7, 98.3(6); C5–C4–C7, 95.5(5); C2–B6–B2, 133.6(3); C2–B6–B5, 128.4(3); C2–B6–B7, 127.7(3); C5–B6'–B2', 132.1(3); C5–B6'–B5', 128.9(3); C5–B6'–B7', 126.6(3).

C4–C7 and B6–B6'–C7 being perpendicular. Both decaborane cages are bound at the exo positions of the norbornyl unit.

Ruthenium-Catalyzed Ring-Opening Metathesis Polymerizations (ROMP) of 6-(5-Cyclooctenyl)-B₁₀H₁₃ (1**) and 6-(5-Norbornenyl)-B₁₀H₁₃ (**2**).** In accordance with previous observations¹⁷ that six-membered rings do not readily undergo ROMP reactions, no ROMP polymerization of 6-(4-cyclohexenyl)-B₁₀H₁₃ (**3**) was observed when it was treated with the Grubbs catalysts, Cl₂Ru(=CHPh)(PCy₃)₂L, L = PCy₃ (**I**) and H₂IMes (**II**), in CH₂Cl₂. However, ROMP of the strained monomers 6-(5-cyclooctenyl)-B₁₀H₁₃ (**1**) and 6-(5-norbornenyl)-B₁₀H₁₃ (**2**) with either **I** or **II** proceeded readily to yield the corresponding poly(6-cyclooctenyldecaborane) (PCD, **6**) and poly(6-norbornenyldecaborane) (PND, **7**) polymers (eqs 6 and 7).



The polymerization reactions were carried out by stirring a mixture of the monomer and catalyst in CH₂Cl₂ at room temperature (for **I**) or under gentle reflux (for **II**). In both

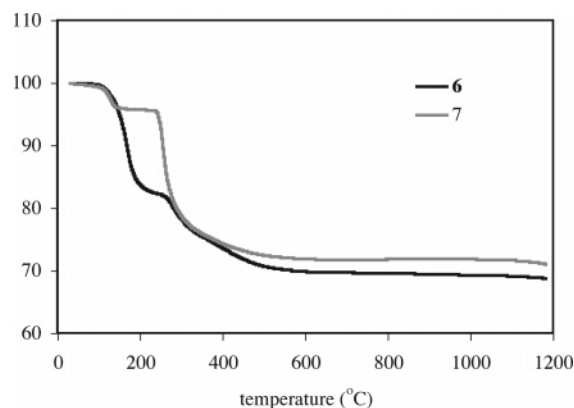


Figure 4. TGA curves of 32 kDa PCD (**6**) and PND (**7**) under argon.

cases, immediate color changes were observed indicating catalyst activation. The solutions became more viscous as the reactions progressed. The reactions were quenched with ethylvinyl ether after 1 h to afford the ether-terminated poly(6-cyclooctenyldecaborane) (PCD, **6**) and poly(6-norbornenyldecaborane) (PND, **7**) polymers. The metal residue was removed by column chromatography on silica gel. The polymer was then precipitated by addition of a concentrated CH₂Cl₂ solution to pentane, leaving behind any unreacted monomer in solution. The polymers were isolated as air-stable off-white solids that were soluble in methylene chloride, THF, and chloroform but insoluble in hexanes or benzene.

The ¹¹B NMR spectra of the polymers again showed patterns characteristic of 6-R-B₁₀H₁₃ derivatives²¹ but with much broader peaks than those of the corresponding monomers. Their ¹H NMR spectra showed, in addition to the resonances of the unsaturated organic backbones, two intensity-two peaks for the two sets of bridging hydrogens on the decaborane cage. Their IR spectra showed the B–H absorption in addition to the vibrations of the unsaturated polymer backbones.

Detailed molecular weight studies were carried out in THF with SEC-GPC employing both multiangle laser light scattering (MALLS) and differential refractive index (DRI) detectors. As shown in Tables 1 and 2, PCD (**6**) and PND (**7**) polymers were readily obtained with *M_n*'s in excess of 30 kDa by employing ~1 mol % of the **II** catalyst. These molecular weights and degrees of polymerization (DP), 141 for PCD and 148 for PND, are significantly higher than those of the previously reported poly(6-hexenyldecaborane) polymers synthesized using Cp₂Zr(CH₃)₂/B(C₆F₅)₃ catalysts (*M_n* ≈ 4 kDa, ~20 DP).³

II showed much higher catalytic activity than **I** for the polymerization of **1**. Thus, for comparable 1 mol % reactions carried out for the same 1 h reaction time, monomer conversion increased from 63.4% to 80.0%, and the degree of polymerization increased from 54 to 141 when **II** was used instead of **I**. On the other hand, both **I** and **II** efficiently polymerized **2**, giving ~90% monomer conversions with comparable degrees of polymerization (145 and 148) for 1 h reactions employing 1 mol % of either catalyst. Since the ring strain of the eight-membered cyclic olefinic substituent of **1** is not as great as that of the bicyclic norbornenyl group

Table 4. Results of Bulk Pyrolyses of PCD (6) (dwell = 1 h)

temp (°C)	ceramic/polymer (g/g)	ceramic yield (%)	B%	C%	H%	B:C	nominal composition
1000	0.33/0.59	55.9	59.94	30.56	0.69	2.18	B ₄ C/C _{0.82}
1200	0.32/0.61	52.4	62.42	30.60	0	2.26	B ₄ C/C _{0.77}
1300	0.28/0.52	53.8	65.86	29.73	0.34	2.46	B ₄ C/C _{0.63}
1400	0.38/0.72	52.7	67.76	28.62	0	2.63	B ₄ C/C _{0.52}
1650	0.33/0.65	50.8	68.80	22.90	0	3.30	B ₄ C/C _{0.21}

Table 5. Results of Bulk Pyrolyses of PND (7) (dwell = 1 h)

temp (°C)	ceramic/polymer (g/g)	ceramic yield (%)	B%	C%	H%	B:C	nominal composition
1200	0.54/0.73	73.9	60.31	32.23	0	2.05	B ₄ C/C _{0.96}
1300	0.44/0.64	68.8	63.40	33.35	0	2.09	B ₄ C/C _{0.92}
1400	0.56/0.79	70.9	64.64	34.47	0.66	2.06	B ₄ C/C _{0.94}
1500	0.44/0.65	67.7	66.14	32.12	0	2.26	B ₄ C/C _{0.77}
1650	0.31/0.53	58.5	67.86	32.24	0	2.34	B ₄ C/C _{0.72}

of **2**, efficient polymerization of **1** required the more active **II** catalyst.

The molecular weights of both polymers could be controlled by the catalyst concentrations. Thus, M_n of the PCD polymer doubled from 6230 to 12 500 when the catalyst concentration of **I** was decreased from ~2 to ~1 mol % (Table 1). Similar increases in molecular weights were observed for the polymerization of **2** upon lowering the concentrations of either the **I** or the **II** catalysts (Table 2). Much higher molecular weight organic polymers have been achieved using even lower catalyst loadings. For example, when employing 500 [M]/[Ru] ratios, the RuCl₂(=CHR')-(PR₃)₂-catalyzed ROMP reactions of 5-cyclooctene afforded polymers with M_n of 111–211 kDa (DP = 1000–1918), while those of 2,5-cyclooctadiene produced polybutadiene with M_n of 57.9–63.2 kDa (DP = 536–585).^{16a} ROMP of 5-norbornene using these catalysts with a 100 [M]/[Ru] ratio afforded polymers with M_n of 31.6–42.3 kDa (DP = 336–450).^{16a} However, our attempts to obtain higher molecular weight PCD and PND polymers with lower catalyst loadings (<1 mol %) led to the formation of insoluble polymeric materials.

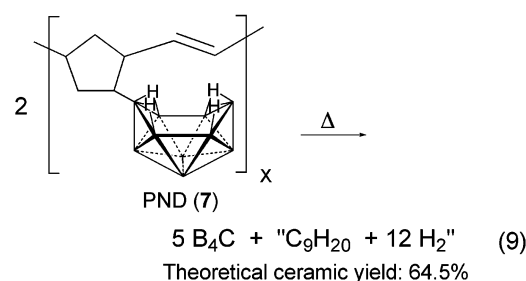
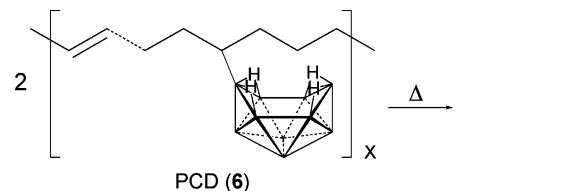
The molecular weights and degrees of polymerization achieved for the PCD and PND polymers are comparable to those found for other inorganic polymers using similar catalyst loadings. For example, Allcock reported that the ROMP of norbornenylphosphazenes bearing ester, phenyl, and alkyl functionalities catalyzed by 1 mol % of **I** generated polymers with degrees of polymerization in the ~40–100 range.¹⁹

When **II** was used as the catalyst, the PDI's of the polymers were higher than those catalyzed by **I**. This result agrees with previous studies of the ROMP of other cyclic olefins using the same catalysts where it was found that, owing to the higher reactivity of **II**, it can "back-bite" at the internal double bonds of the polymer to give secondary metathesis leading to the formation of cyclic polymer structures and, accordingly, an increase in polydispersity.²³

Ceramic Conversion Reactions of Poly(6-cyclooctenyl-decaborane) (PCD, 6) and Poly(6-norbornenyldecaborane) (PND, 7). Boron carbide is normally represented by a B₄C (B₁₂C₃) composition with a structure based on B₁₁C icosahedra and C–B–C intericosahedral chains, but single-

phase boron carbides are also known with carbon concentrations ranging from 8.8 (~B_{10.5}C) to 20 (~B₄C) at. %.¹ This range of concentrations is made possible by the substitution of boron and carbon atoms for one another within both the icosahedra and the three-atom chains.

Because of their high carbon contents, the PCD and PND polymers would be expected to produce the more carbon-rich B₄C composition. Thus, if all of the boron in the PCD and PND polymers was retained and all of the hydrogen and excess carbon was lost during their ceramic conversion reactions, then PCD and PND would convert to a B₄C boron-carbide composition according to eqs 8 and 9 with theoretical char yields of 60.0% and 64.5%, respectively.



As shown in Figure 4, thermogravimetric analysis (TGA) of ~32 kDa samples of **6** and **7** showed that the polymers were stable up to 120 (PCD) and 150 °C (PND). Modulus differential scanning calorimetry (DSC) studies also showed that the glass-transition temperatures (T_g) of both polymers were between 65 and 70 °C. The fact that their T_g s are lower than their initial decomposition temperatures is important since it allows polymer processing into desired shapes before thermal conversion to the final ceramic materials.²⁴

According to the TGA analysis, PCD showed an initial 18% weight loss between ~150 and 220 °C followed by a

(23) Bielawski, C. W.; Grubbs, R. H. *Angew. Chem., Int. Ed.* **2000**, 39, 2903–2906.

(24) See, for example: Welna, D. T.; Bender, J. D.; Wei, X.; Sneddon, L. G.; Allcock, H. R. *Adv. Mater.* **2005**, 17, 859–862.

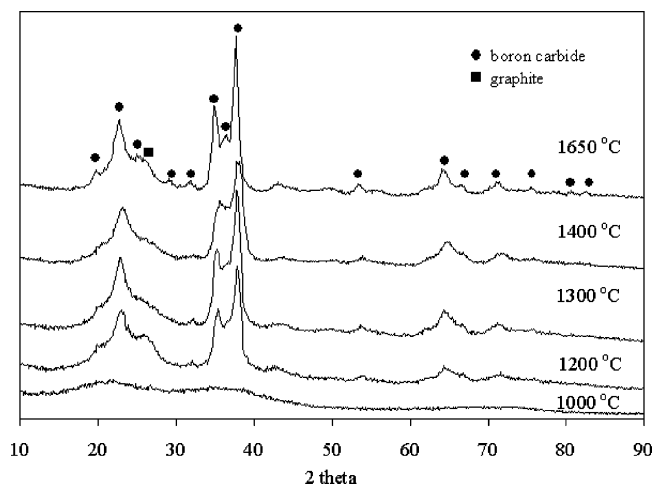


Figure 5. XRD patterns of the PCD (6)-derived ceramic chars at different temperatures.

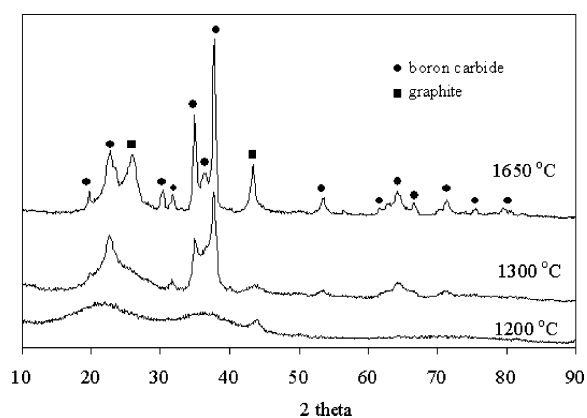


Figure 6. XRD patterns of the PND (7)-derived chars at different temperatures.

second loss starting at ~ 350 °C. This second loss was essentially complete by 800 °C to give a char yield of 70%. PND showed a similar two-step weight loss pattern beginning at 120 and 180 °C, respectively, with the second loss complete by 500 °C to give a 72% char yield. The higher than predicted char yields for both polymers indicate additional carbon was retained in the ceramic.

Bulk ceramic conversions of ~ 32 kDa samples of the polymers were carried out under an argon purge. The char yields (Table 4) of the bulk pyrolyses of PCD remained nearly constant (51–56%) over the 1000–1650 °C range but were lower than both the theoretical and TGA values. The 70% bulk char yields (Table 5) of PND up to 1500 °C were consistent with the TGA value, but the char yield dropped to 58% at 1650 °C.

The elemental analyses showed that all ceramic chars had B:C ratios lower than the 4:1 ratio of B_4C , indicating the presence of excess carbon. The presence of free carbon in the 1650 °C chars was also confirmed by their Raman spectra, which showed, in addition to the boron-carbide bands²⁵ at 477, 533, 728, and 1094 cm^{-1} , intense carbon bands at 1344 and 1594 cm^{-1} .²⁶

The observed 3.30 and 2.34 B:C ratios of the 1650 °C chars of PCD and PND correspond to nominal compositions of $B_4C/C_{0.21}$ and $B_4C/C_{0.72}$, respectively. The high carbon content of these ceramics is consistent with the carbon-rich

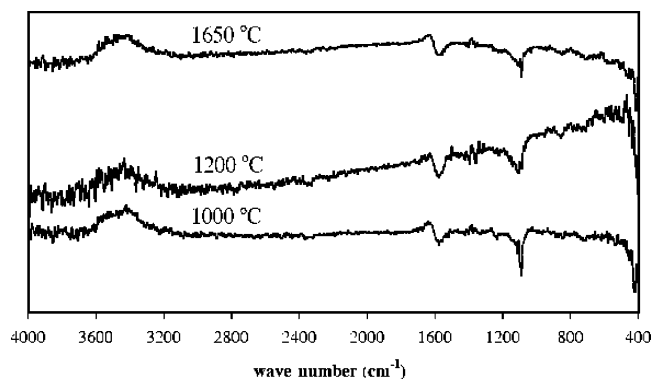


Figure 7. DRIFT spectra of the ceramic chars obtained from PND (7) at different temperatures.

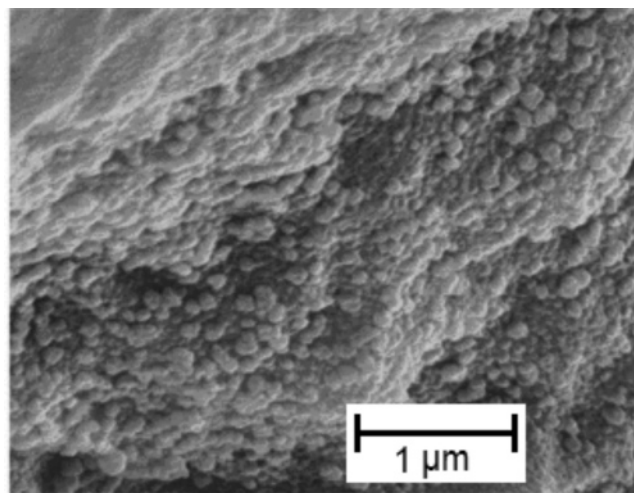


Figure 8. SEM image of the ceramic char obtained from the pyrolysis of PND (7) at 1650 °C.

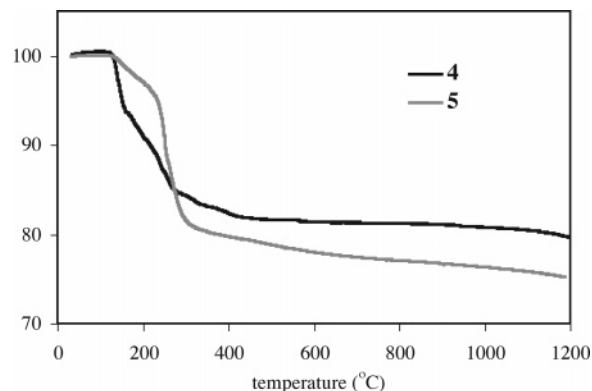


Figure 9. TGA curves of 4 and 5 in argon ramped at 10 °C/min.

nature of the PCD and PND polymers, but differences in polymer structure also play an important role in carbon retention. Previous studies have clearly shown that pre-ceramic polymers containing ring structures effectively retain ring elements during ceramic conversions. Thus, even though the PND polymer has a slightly higher B:C ratio (B:C = 10:7) than the PCD polymer (B:C = 10:8), elemental analyses demonstrated that the PND-derived chars have significantly higher carbon content than the analogous PCD chars. This difference can clearly be traced to the different backbone structures of the two polymers: PCD has a linear backbone containing one double bond, while PND has a ring/double-bond backbone. Both the PCD- and PND-derived

Table 6. Results of Bulk Pyrolyses of 4

temp (°C)	dwelt (h)	precursor/ceramic (g/g)	char yield (%)	B%	C%	H%	B:C	nominal composition
1000	1	0.42/0.60	70.0	82.22	16.74	0.83	5.46	B _{5.46} C
1200	1	0.34/0.53	64.2	83.82	15.86	0.45	5.87	B _{5.87} C
1650	1	0.33/0.59	55.9	81.81	18.50	0	5.05	B _{5.05} C
1650	8	0.23/0.43	53.5	80.26	19.84	0	4.62	B _{4.62} C

Table 7. Results of Bulk Pyrolyses of 5

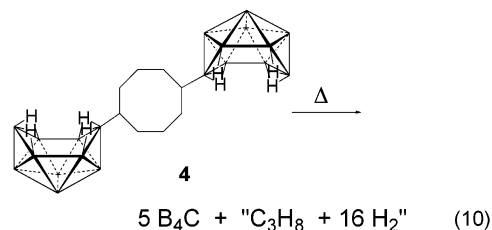
temp (°C)	dwelt (h)	precursor/ceramic (g/g)	char yield (%)	B%	C%	H%	B:C	nominal composition
1000	1	0.40/0.51	78.4	80.28	15.61	0.47	5.88	B _{5.88} C
1200	1	0.40/0.53	75.5	83.36	16.59	0	5.74	B _{5.74} C
1650	1	0.35/0.52	67.3	81.93	17.60	0	5.32	B _{5.32} C
1650	10	0.28/0.54	51.8	79.92	20.51	0	4.32	B _{4.32} C

ceramics showed higher carbon content than the ceramics (B:C = 4.05) obtained from the poly(6-hexenyldecaborane) polymer. The poly(6-hexenyldecaborane) polymer has both a higher B:C ratio (10:6) and a saturated linear hydrocarbon backbone that is more easily eliminated during the ceramic conversion process.³

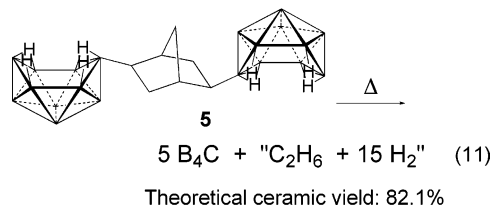
As shown in Figures 5 and 6, powder X-ray diffraction (XRD) studies showed that the 1000 °C chars of both polymers were amorphous. Nevertheless, their diffuse reflectance infrared Fourier transform (DRIFT) spectra (Figure 7) showed boron-carbide bands near ~1100 and ~1600 cm⁻¹,²⁷ indicating that boron carbide had already formed in these chars before its crystallization. The absence of any B–H and/or C–H vibrations in the DRIFT spectra also demonstrates that there were no significant amounts of chemically active polymeric fragments remaining in the chars pyrolyzed at 1000 °C.

While still retaining a substantial amorphous component, chars obtained at higher temperatures showed the boron-carbide diffraction peaks²⁸ along with the graphite peaks at 26° and 42° 2 θ . For PND-derived ceramics, the onset of boron-carbide crystallization occurred between 1200 and 1300 °C. This is higher than for the PCD- and poly(6-hexenyldecaborane)-derived ceramics, where initial boron-carbide crystallization occurred between 1000 and 1200 °C.³ The excess carbon in the PND chars undoubtedly retards the boron-carbide crystallization. Because of the excess carbon, the PND-derived ceramic chars also exhibited low densities even at 1650 °C (2.20 g/cm³). In agreement with the XRD results, the SEM images of the 1000 °C PCD and PND ceramic chars appeared amorphous, while their 1650 °C chars showed nanocrystallites embedded in a largely amorphous matrix (Figure 8).

Ceramic Conversion Reactions of 6,6'-(1,5-Cyclooctyl)-(B₁₀H₁₃)₂ (4) and 6,6'-(2,5-Norbornyl)-(B₁₀H₁₃)₂ (5). Given their higher B:C ratios, both **4** (20:8) and **5** (20:7) would be expected to generate boron-carbide ceramics containing less free carbon than the PCD and PND precursors. Assuming that all of the boron in these precursors is retained during the ceramic conversion and that the hydrogen and excess carbon is lost, then **4** and **5** would convert to boron-carbide ceramics according to eqs 10 and 11 to give 78.4% and 82.1% char yields, respectively.



Theoretical ceramic yield: 78.4%



Theoretical ceramic yield: 82.1%

As illustrated in the TGA curves in Figure 9, **4** and **5** were stable in argon up to 150 °C. The ceramic conversions for both compounds occurred in one step and were complete by 600 °C to give TGA char yields of 82% and 76% at 1200 °C. However, during the bulk pyrolyses (Tables 6 and 7) of **4** and **5** carried out under an argon purge, both precursors showed additional weight losses at temperatures beyond the TGA range with char yields at 1650 °C of 53.5% for **4** and 51.8% for **5** (heated for 8 and 10 h, respectively). Elemental analyses showed that significant amounts of hydrogen remained in the 1000 °C-**4** (0.83 wt % or 0.59 equiv per carbon), 1200 °C-**4** (0.45 wt % or 0.34 equiv per carbon), and 1000 °C-**5** (0.47 wt %, or 0.36 equiv per carbon) ceramic chars but not in their high-temperature chars. This suggests incomplete ceramic conversions at the lower temperatures with retention of some chemically active species. These species were then lost at the higher pyrolysis temperatures, resulting in the observed weight losses.

Although compound **4** has a lower B:C ratio than **5**, the elemental analyses showed that the **4**-derived chars had a higher B:C ratio than the **5**-derived chars (B:C = 4.62 for **4** and 4.32 for **5**) as a result of the norbornyl bicyclic ring structure of **5** retarding the loss of carbon during ceramic conversion. Both ceramics have lower B:C ratios than the ceramics (B:C ~7:1) derived from 6,6'-(CH₂)₆-(B₁₀H₁₃)₂. The difference arises because the 6,6'-(CH₂)₆-(B₁₀H₁₃)₂ precursor has both a higher B:C ratio (B:C = 20:6) than **4** or **5** and a linear structure for the hydrocarbon chain bridging the two cages that facilitates carbon loss.³

XRD analyses (Figures 10 and 11) showed that boron-carbide crystallization for both the **4**- and **5**-derived ceramics

(25) Tallant, D. R.; Aselage, T. L.; Campbell, A. N.; Emin, D. *Phys. Rev. B* **1989**, *40*, 5649–5656.

(26) Tuinstra, F.; Koenig, J. L. *J. Chem. Phys.* **1970**, *53*, 1126–30.

(27) Becher, V. H. J.; Thevenot, F. *Inorg. Allg. Chem.* **1974**, *410*, 274.

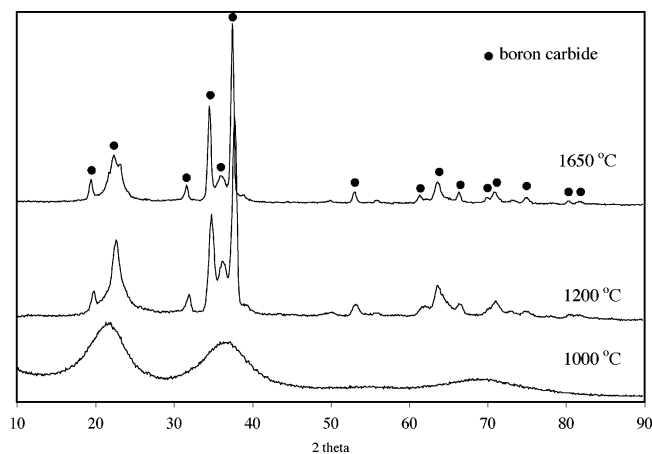


Figure 10. XRD patterns of the **4**-derived ceramics at different temperatures.

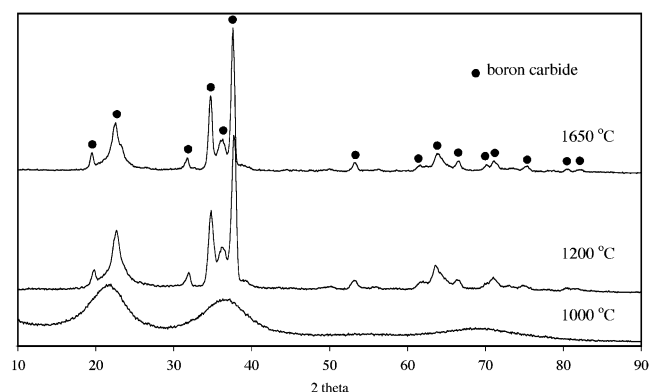


Figure 11. XRD patterns of the **5**-derived ceramics at different temperatures.

began between 1000 and 1200 °C. The boron-carbide diffraction peaks²⁸ are clearly evident in the 1650 °C chars, and these peaks are much more narrow than those of the PCD and PND chars at this temperature. Thus, the absence of a significant carbon phase in the **4**- and **5**-derived ceramics facilitates a higher degree of boron-carbide crystallization. The full-width at half-maximum (fwhm) of the peaks at 37.5° 2 θ for both the 1650 °C **4**- and **5**-derived chars corresponded to ~ 100 nm crystal sizes. This is consistent with the SEM analyses of these chars that showed ~ 100 nm boron-carbide crystals embedded in an amorphous phase. In agreement with the elemental analyses, the energy-dispersive spectrum (EDS) of the **5**-derived 1650 °C chars showed boron and carbon peaks in relative intensities of $\sim 5.4:1$.

Also consistent with the elemental analyses, the 26° 2 θ carbon diffraction peak found in both the PCD- and PND-derived chars was not observed in the XRD of the **4**- and

5-derived ceramics. Likewise, while the Raman spectrum of the 1650 °C **5**-derived char still showed, in addition to the boron-carbide peaks,²⁵ the carbon 1344 and 1594 cm^{-1} bands,²⁶ they were greatly reduced in intensity compared to the spectra of the **6**- and **7**-derived chars discussed earlier.

The density of the 1650 °C **5**-derived ceramic (2.45 g/cm^3) was close to the theoretical value of boron carbide at 2.52 g/cm^3 and much higher than that measured for the PND char (2.20 g/cm^3) at this temperature. The higher density compared to the PCD- and PND-derived chars is a result of both the absence of a significant amount of the less-dense carbon phase and the enhanced boron-carbide crystallization.

Conclusions

The results presented above clearly demonstrate that ruthenium-catalyzed ROMP reactions are important new methods for the systematic formation of poly(organodecaborane) polymers. Polymers **6** and **7**, as well as the new organodecaborane linked-cage molecular compounds **4** and **5**, have proven to be excellent single-source precursors to boron-carbide/carbon ceramic materials with controlled compositions. The poly(6-cyclooctenyldecaborane) and poly(6-norbornenyldecaborane) have much higher molecular weights than any previously reported poly(organodecaborane) polymers. As a result, they exhibit an improved processability that should now enable many applications not heretofore possible. For example, we recently demonstrated²⁴ that poly(6-norbornenyldecaborane) can be electrostatically spun to produce nano- to microscale polymer fibers which, upon pyrolysis, convert to boron-carbide fibers. Finally, since the ruthenium-based ROMP catalysis works with a wide variety of functionalized olefins, these reactions have excellent potential for the production of much more complex poly(organopolyborane) polymers and copolymers than possible with our previously reported zirconium-catalyzed alkenylpolyborane polymerizations.

Acknowledgment. We thank the Air Force Office of Scientific Research, the U.S. Department of Energy, Office of Basic Energy Sciences, and the National Science Foundation for support of this project. We also thank Dr. Gary L. Wood and Prof. Robert T. Paine at the University of New Mexico for their assistance with DRIFT spectroscopy, Dr. Jeffrey A. Ahlgren for assistance in setting up the GPC system, and Kris Behler at the Department of Materials Science and Engineering at Drexel University for assistance with Raman Spectroscopy.

Supporting Information Available: CIF files for **2**, **3**, and **5**. This material is available free of charge via the Internet at <http://pubs.acs.org>.

(28) Aselage, T. L.; Tissot, R. *J. Am. Ceram. Soc.* **1992**, *75*, 2207–2212.